

An Instantaneous-Profile Laser Scanner to Measure Soil Surface Microtopography

Frédéric Darboux* and Chi-hua Huang

ABSTRACT

Soil surface roughness affects overland flow and soil erosion processes, yet studies on roughness effects are hampered by the difficulty of acquiring microtopographic data. The purpose of this study is to develop an instantaneous surface-profile laser scanner that has significantly higher data acquisition rate and smaller overall size than previous laser scanners. This laser scanner consists of two diode lasers and a digital camera mounted on a single rail. The lasers project a bright line on the surface and the shape of this line, digitized by the camera from an oblique angle, changes depending on the surface microtopography. From the geometry of the laser-camera assembly, the line image is converted to surface heights using a calibration procedure based on a triangulation principle. A computer drives the translation of the laser-camera assembly along the rail, processes the images from the camera, and records the surface profile data during the scan. This ensures the reconstruction of the surface morphology by juxtaposing successive profiles. The current system can measure the microtopography of a 50 cm by 4 m surface with a positional and elevational accuracy of 0.5 mm. The scanner can digitize six surface profiles per second. This translates to a time of 7.4 min to scan a 4-m long section with profiles taken every 1.5 mm apart. The instantaneous-profile laser scanner is significantly faster than previous scanner technologies and allows new research opportunities in quantifying surface boundary processes, such as soil erosion.

THE ACQUISITION of soil surface microtopography data is normally achieved by using stereophotography (Warner, 1995; Zribi et al., 2000), contact probes (Kuipers, 1957; Whalley and Rea, 1994), or laser scanners. Laser scanners using different operational principles have been developed to convert the optical measurements into surface height readings.

Scanners reported by Römkens and Wang (1987) and Huang et al. (1988) used triangulation to measure surface elevation. A laser beam was projected vertically onto the surface and a line camera detected the light spot reflected from the surface. Because of the fixed camera-laser geometry, the surface height was estimated using a simple calibration procedure. Missing values were encountered in triangulation-based laser scanners because some part of the surface blocked the view of the laser point from the camera (shadow effect). This shadow effect could be minimized by either using two cameras in opposite view angles or rotating a single camera 180° to achieve the same dual camera effect. Even this still left some unmeasured points (Römkens and Wang, 1987).

To overcome the undesirable shadow effect, scanners with both emitter and receiver placed along the same

optical axis were designed. These systems used the defect-of-focus method (Bertuzzi et al., 1990) or measurement of wave curvature (Kamphorst, 2000; Imagine Optic, 2001). Whatever the technique used, all these laser scanners have the drawback of measuring surface elevation one point at a time, making the measurement over a surface relatively time-consuming. Another disadvantage of the point-based laser scanner is the need to construct a two-dimensional traversing frame to map the height changes for a surface. This traversing frame is costly to built and cumbersome to use, especially for field situations. A laser scanner measuring several points at a time was first reported by Rice et al. (1988). Because of its design, it did not measure instantaneously the surface elevations along a linear transect, making the data processing more complicated. The laser scanner recently presented by Wilson et al. (2001) is indeed capable of measuring a surface profile instantaneously. Nevertheless, the advantage of using a flexible frame that could be assembled over a large plot (i.e., 2.4 by 9.1 m) becomes a drawback in measurement accuracy because the supporting frame was supposed to provide the reference plane for the elevation measurement. This is why most scanners were constructed with a rigid frame to maintain a constant reference plane for the desired millimeter scale elevational and positional accuracy.

Additionally, the line scanner reported by Wilson et al. (2001) is, in fact, slower and less accurate than the point-scan system reported by Flanagan et al. (1995), which was modified from the Huang and Bradford (1990) system. The system of Flanagan et al. (1995) can digitize a 2.5-m profile at 0.5-mm grid in 20 s (approx. 15 000 readings per minute) with a 0.5-mm positional and elevational accuracy.

The purpose of this study is to develop a laser scanner with higher data-acquisition rate and smaller overall size than previous laser scanners. This paper describes a new laser scanner for measuring instantaneously the heights along a surface profile. This feature, combined with up-to-date camera and computer technology, considerably speeds up the measurement as compared with previously reported laser scanners. Because the measuring device is moved along a single rail, design and transport of this system are simplified. However, using the triangulation principle, it does not overcome the shadow effect. Our instantaneous-profile laser scanner has been in operation since September 1999 in both laboratory and field experiments. Several units have already been built and used successfully in different laboratories.

Abbreviations: CCD, charge-coupled device; DEM, digital elevation model.

F. Darboux, Purdue University; presently at: INRA-Science du sol, B.P. 20619, F-45166 Olivet Cedex, France; C. Huang, USDA-ARS, National Soil Erosion Research Laboratory, 1196 Soil Bldg., Purdue University, West Lafayette, IN 47907-1196. Received 28 Nov. 2001.
*Corresponding author (Frederic.Darboux@orleans.inra.fr).

MATERIAL AND METHODS

Principles of Surface Profile Detection

The instantaneous-profile laser scanner uses the triangulation principal to measure the point coordinates along a profile. Triangulation has already been used by some of the point laser scanners earlier (Römkens and Wang, 1987; Huang and Bradford, 1990). The previous design used a laser to project a bright spot on the surface. A charge-coupled device (CCD) line camera was aligned with the optical axis of the laser beam. The CCD cells detected the laser spot reflected from the surface because of its greater light intensity. The reflected laser spot is the one having the greater light intensity. Depending on the elevation of the surface, the bright spot was registered by a set of different CCD cells. Using a calibration procedure, the CCD coordinate was converted to a height coordinate. To map the surface heights, the laser camera unit was moved on a traversing frame in both horizontal directions.

The instantaneous-profile laser scanner uses the same principle, but a laser line and a CCD-array camera are used. The laser generates a narrow line of intensive light on the surface. This line is in the field of view of the CCD-array camera from an oblique angle. The profile can be characterized on the CCD array by a series of cells receiving a high flux of laser light. A calibration procedure converts the CCD coordinates (row and column) to spatial coordinates (x and z) and produces instantaneously the height variations along a profile. To map the surface heights, successive profiles are recorded as the laser-camera assembly is moved automatically along a rail.

Similar to the point-scan system, the elevation range, width of the profile, and spatial resolution are dependent on the laser-camera geometry, the size of the CCD array, and the focal length of the lens.

System Design

Hardware

To ensure a sufficient light intensity of the laser line, two laser diode modules are used. Each laser diode generates a 3.60-mW beam at 635 nm (red). Laser beams are split into a 60° fan by a prism. Laser diodes are mounted 40 cm apart and lined up to generate a single 0.5-mm wide line on the targeted surface. The use of two lasers also improves the continuity of the line of light on the surface because it decreases the shadow effect because of the interception of the laser light by high elements of the topography. The length of

the laser line was adjusted to exceed slightly the field of view of the camera.

An 8-bit monochrome CCD camera with 1030 rows and 1300 columns and a 9-mm lens is used to detect the laser line. The camera is connected to a computer through a frame grabber, that is, a computer interface for picture acquisition. A red filter is attached to the lens to increase the contrast of the laserline image in the field of view of the camera.

The lasers and camera are mounted on a carriage assembly (Fig. 1). To allow the alignment of the laser beams, the laser modules are inserted in ball mounts (15° rotation in all directions). The camera is attached to a tilting mount so that the view angle can be adjusted. Ball and tilting mounts are secured tightly to a rigid support to ensure a stable geometry of the camera laser assembly. The carriage is mounted on a 4-m long rail and is driven by a stepping motor via a toothed belt incorporated into the rail. A computer program and a custom-built electronic board perform the control of the carriage movement and the picture acquisition and processing. Two microswitches are attached at both ends of the rail and connected to the electronic board to stop the carriage movement if it accidentally reaches one of the rail ends.

Operation

After the laser scanner is positioned over the surface to be measured, a dedicated software controls the scanner operation. Input parameters include travel length, direction of carriage movement, and the image threshold value used to identify the laser profile in the picture. The threshold value depends on the ambient light, the color of the surface, and the laser intensity. An accessory program is used to select the threshold value.

The scanner control program interacts through a digital input-output interface with the electronic board, which generates the stepping pulses for the stepper motor and a trigger signal for picture acquisition. The stepper motor driver is capable of microstepping up to 51 200 microsteps per revolution. By knowing the size of the motor gear, we can calculate the number of microsteps n required to move a fixed distance. A picture acquisition signal is sent to the frame grabber every n microsteps of the motor, ensuring a constant distance between each profile acquisition. The number of microsteps between two successive profile readings can be modified using microswitches on the electronic board. This feature allows the user to change the spacing between profiles.

The micro-stepping signal frequency, or timing between

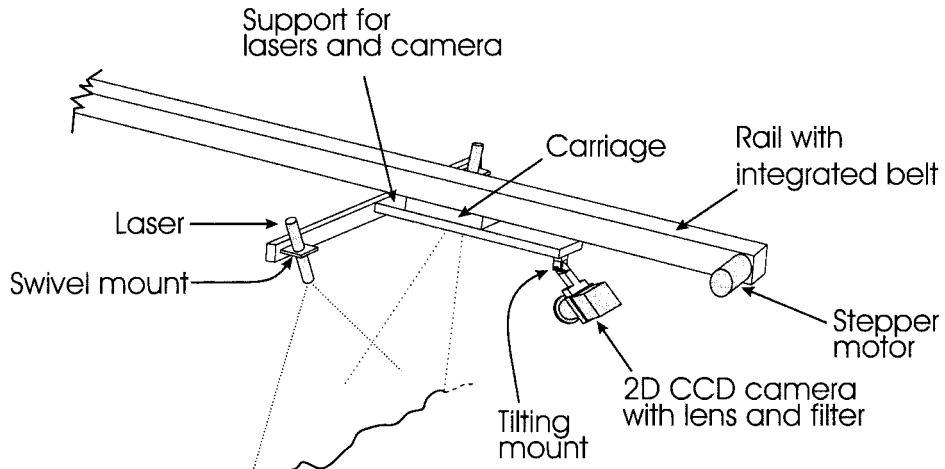


Fig. 1. Layout of the instantaneous profile laser scanner.

microsteps, can be adjusted using a variable resistor. This adjustment affects the speed of the carriage and is set such that the computer can acquire and process the pictures in real time without missing any profile. Because the picture acquisition signal depends directly on the micro-stepping signal, changes in the carriage speed do not affect the distance between profiles.

When a picture is acquired, the software attempts to identify the location of the laser line. The detection of the laser line works similarly to the scanner system used by Huang et al. (1988), except that the new system processes CCD information digitally by software while the old system processed the CCD signal by analog hardware circuitry. Because of the 8-bit resolution of the acquired image, each pixel has a gray scale value between 0 (black) and 255 (white).

The profile identification is performed using a two-step process. First, the picture is binarized; all pixels with a value above the predefined threshold value are selected because they potentially belong to the laser-line image. The other pixels are discarded. Then, questionable pixels are removed. Among the selected pixels, some could be artifacts because of either specular reflection from the soil surface or elements not belonging to the soil surface such as overhanging grass blades. The program records, in each column of the picture, the location of the first and the last preselected pixels, or pixels above the threshold value. The laser spot is considered as identified if these pixels are spaced by <10 pixels (note: this value can be changed in the software configuration file). In that case, for the considered column, the row indices of the first and last pixels are summed and this sum is stored in memory. Otherwise a missing-data label is stored.

Summing the first and last row indices over the detection threshold provides an equivalent of half-pixel resolution while still working with integer numbers. For each analyzed picture, a single numeric value corresponding to the location of the laser line is saved per column. It means that 1300 values are saved for each picture. Compared with the 1.3 million pixels of a picture, the real time processing reduces drastically the amount of information to be stored.

With the current hardware and software, the acquisition and processing of one picture takes 0.16 s. This leads to an acquisition rate of six profiles per second (7800 height measurements per second). This translates to a total time of 7.4 min to scan a 4-m long section with profiles taken 1.5 mm apart.

Data Processing

Calibration Procedure

The output file of the laser-scanner software contains information about the location of the profile on each of the pictures. The conversion from pixel coordinates to spatial coordinates is performed afterwards. In the following discussion, x , y , and z defines an orthogonal reference with z the height axis, y the axis parallel to the rail and x in the plane of the laser.

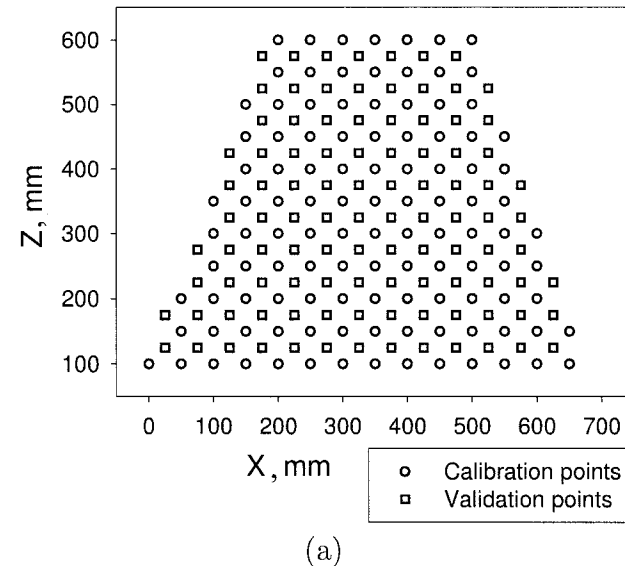
Because the profiles are saved in the order of acquisition and the distance between successive profiles is constant, the determination of the y coordinate is straightforward. Estimations of x and z are performed using a dedicated calibration procedure. The calibration consists of measuring a set of points of known x and z coordinates located in the laser plane. For each calibration point (x, z) in the laser plane, we measure the corresponding column and row (c, r) in the picture frame. A two-dimensional polynomial regression is then performed. Polynomial functions have been classically used in photogrammetry to adjust pictures for lens and view angle and restitute original ground geometry (Buiten, 1993). In principle, the

calibration performed here is identical to the geometry correction used in processing aerial and satellite pictures. Some testing showed a fourth-order polynomial was needed to account for the nonlinearity:

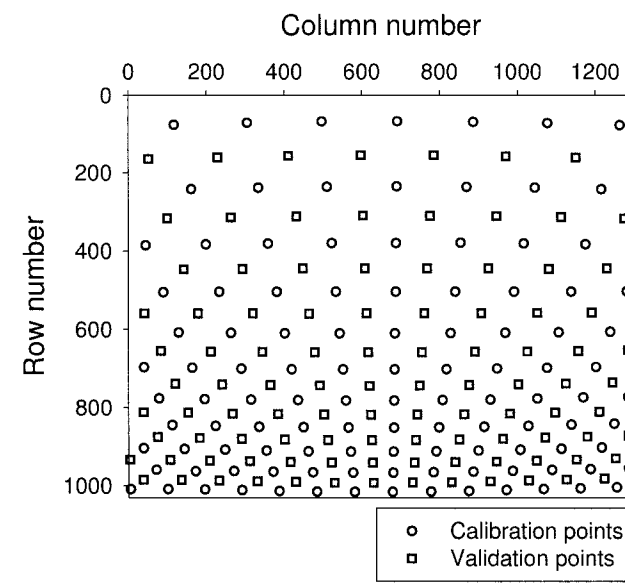
$$\begin{aligned} x = & A_{15}c^4 + A_{14}r^4 + A_{13}c^2r^2 + A_{12}c^3r + A_{11}cr^3 + \\ & A_{10}c^3 + A_9r^3 + A_8cr^2 + A_7c^2r + A_6c^2 + \\ & A_5r^2 + A_4cr + A_3c + A_2r + A_1 \end{aligned} \quad [1]$$

$$\begin{aligned} z = & B_{15}c^4 + B_{14}r^4 + B_{13}c^2r^2 + B_{12}c^3r + B_{11}cr^3 + \\ & B_{10}c^3 + B_9r^3 + B_8cr^2 + B_7c^2r + B_6c^2 + \\ & B_5r^2 + B_4cr + B_3c + B_2r + B_1 \end{aligned} \quad [2]$$

The calibration is usually performed before the measurement. First, the rail is aligned horizontally. The lasers are focused and lined up in the same vertical plane. The calibration



(a)



(b)

Fig. 2. Position of calibration and validation points viewed by the camera in (a) the (x, z) geometric coordinate, and (b) (column, row) camera pixel coordinate.

points are defined by a 5-cm square grid printed on a large sheet of paper taped to a 6-mm thick glass plate, and set in the laser plane. In the center of each square, a cross was printed to define a validation point. A picture is taken with the camera. The sets for calibration and validation are built from the picture by noting the coordinates of each point in the picture reference (c, r) and in the laser plane (x, z) (Fig. 2). The regression is then performed on the calibration points and validated using the validation points.

Digital Elevation Model Construction

After the output file from the laser scanner is processed using the calibration polynomials, a set of (x, y, z) coordinates is obtained. To obtain a digital elevation model (DEM), the points have to be spaced over a regular x and y grid.

By design, the measured points are regularly spaced along y between profiles. Within each individual profile, points are not regularly spaced because of the combination of nonlinearity and height changes along a profile. A simple procedure was used to obtain a regular grid. Knowing the targeted grid spacing along x , the height of each measured point is attributed to the closest point on the grid. If several measured values are attributed to the same grid point, the mean height is recorded. If no measured point is attributed to a particular grid point, a missing-data label is marked at this particular location.

RESULTS AND DISCUSSION

Performance Assessment

Calibration

In the current configuration, the scanner is capable of measuring instantaneously a 50-cm long profile every 1.5 mm. For this purpose, the camera has a 9-mm lens and is setup at a 45° angle from the rail.

A calibration was performed using 111 calibration points and 101 validation points. Figure 3 compares the actual location of these points on the (x, z) plane with the estimated location calculated from the calibration coefficients. The general agreement between actual and estimated locations, for both calibration and validation points, indicates the quality of the calibration procedure. The points at the corners of the picture have the largest deviations because they are located on the border of the interpolation area and because the deformation of the (x, z) plane is greatest at the corners.

Using the calibration coefficients, we estimate the (x, z) value corresponding to each pixel and the size of the

- Calibration points - measured
- Calibration points - estimated
- Validation points - measured
- Validation points - estimated

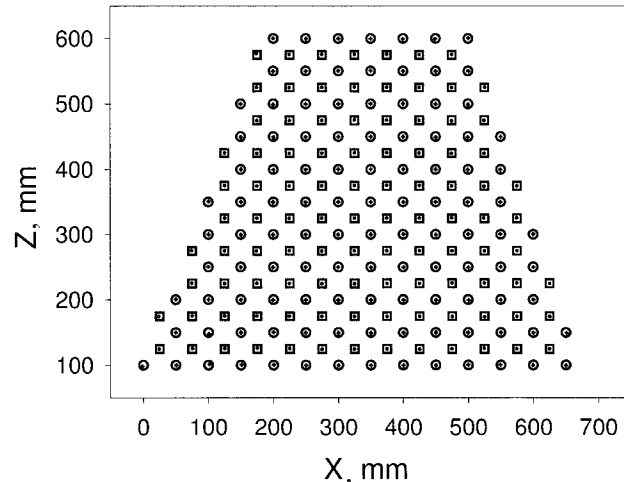


Fig. 3. Position of the measured and estimated points in the laser-beam plane for the calibration and validation points.

area imaged by each pixel, that is, the spatial resolution of the instantaneous-profile laser scanner Fig. 4.

By summing the resolutions along x and z , we calculated also the width of the profile (Fig. 4a, scale located on the right side of the graph) and its height (Fig. 4b, scale located on the right side of the graph). The resolution degrades from the top to the bottom of the picture because the distance between the lens and the (x, z) plane increases. The spatial resolution is more variable for z (that is, 0.23–1.1 mm) than for x (that is, 0.24–0.57 mm) because the camera is tilted downward. The total range of heights of the picture is equal to 53.2 cm. For a targeted vertical resolution of 0.5 mm, the scanner can instantaneously measure a 47-cm long profile. For a height range of 15 cm, the vertical resolution is between 0.4 and 0.6 mm.

The accuracy of calibration procedure can be calculated from the distance between actual and estimated validation points. To give more meaning to the accuracy estimation, we computed the ratio between the accuracy and the resolution for each calibration and validation point in the x and z directions (Fig. 5). Using this normal-

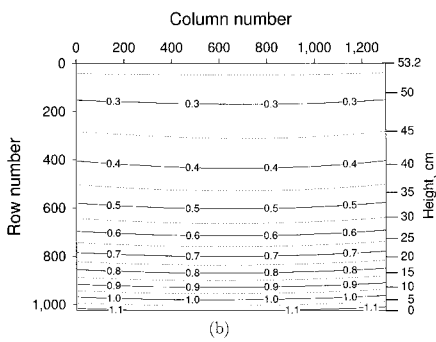
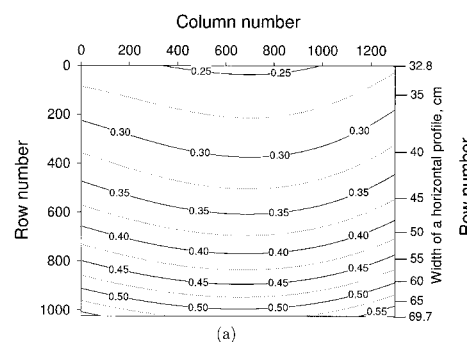


Fig. 4. Resolutions of the laser scanner in millimeters, shown as contours, for (a) horizontal direction (with width of the profile) and (b) vertical direction (with height of the profile from the bottom edge of the picture).

ization, a ratio of one means that the accuracy is equal to the spatial resolution. In all four cases, the mean and median values are lower than one. More than 75% of the points have a ratio lower than one. Therefore, we can conclude that the accuracy of the measurement is better than or close to the spatial resolution in more than 75% of cases. It also means that the calibration procedure takes advantage of the large number of pixels of the CCD array. The similarity of the accuracy resolution ratios between the calibration and validation points indicates the point's density on the (x, z) plane is sufficient.

Measurement Reproducibility

The condition of the measurement also affects the performance of the device. We first evaluated the sensitivity of the measurement when the camera was stationary (static noise). We then determined the reproducibility of the positioning with the carriage movement activated.

Static noise. To quantify the static noise, a horizontal flat target was digitized one thousand times without any

carriage movement. The profiles were extracted using the usual identification procedure. For each column of the CCD array, we calculated the standard deviation of the row index over the 1000 samples. The test was first performed at the regular acquisition rate of 6.5 Hz. To evaluate the drift in the measurement with time, a similar procedure was performed at 0.16 Hz (one frame every 6.5 s). In both cases, the mean standard deviations are lower or equal to one twentieth of a pixel and the maximum standard deviation lower than half a pixel (Fig. 6). The results show that the laser scanner has a very low static noise and no significant drift.

Positioning. The reproducibility of the positioning was evaluated using a pair of sloping flat surfaces at a preset distance apart. An inaccurate positioning will cause a deviation in the measured heights. Knowing the slope of the target surfaces, the horizontal shift could be calculated. The test was performed for traveled distances of 0.9, 1.8, 2.7, and 3.8 m. For each selected distance, the starting and ending profiles were taken 10 times with the carriage moving in both forward and reverse directions. To ensure independence between

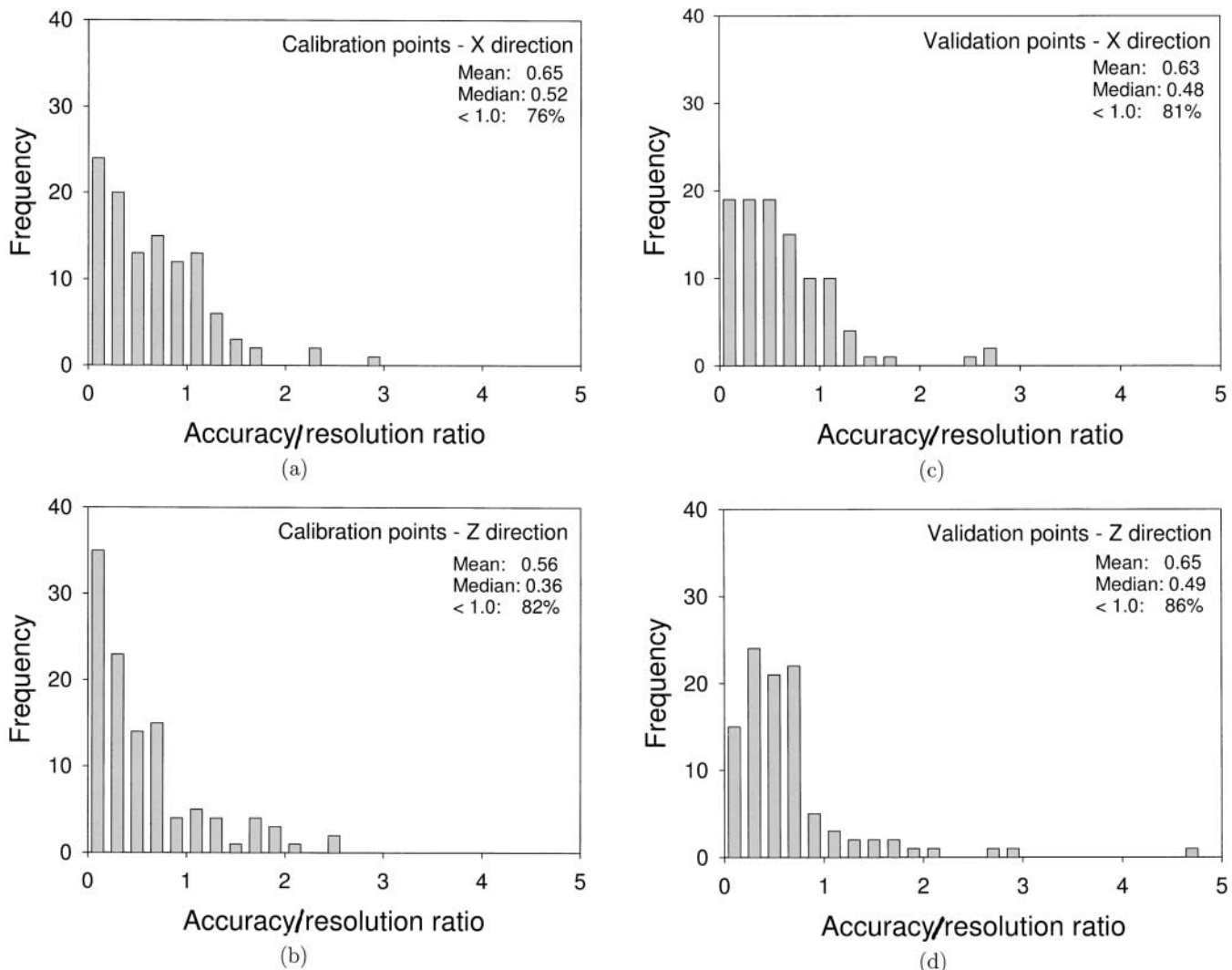


Fig. 5. Frequency distribution of the accuracy/resolution ratio for the calibration (a and b) and validation (c and d) points in the x and z directions.

the replicates, at the end of each scan, the motor was deenergized, the carriage was manually moved away, and then put back to its starting position.

Table 1 presents the standard deviations of the positioning. The positioning does not depend on either the scan direction or the travel distance. It shows a consistent position reproducibility of half a millimeter.

Measurement Accuracy

Absolute accuracy. To estimate the absolute accuracy of the laser scanner, we measured a block having a stairlike shape. This block was a metal plate with a total of 51 steps of 5 mm in height. Since the block was cut with a mill, its accuracy was better than 0.1 mm. The height of the target was adjusted so that the center step is lined up with the z resolution of 0.5 mm. For the whole 250 mm range, the measured heights are in good agreement with the target shape, considering the vertical resolution is close to 0.5 mm (Fig. 7a). The test was conducted 1 mo after calibration, showing a stable performance with time.

Relative accuracy. Scanning the same soil surface from two opposite directions assessed the relative accuracy. Between the two scans, the laser scanner was ro-

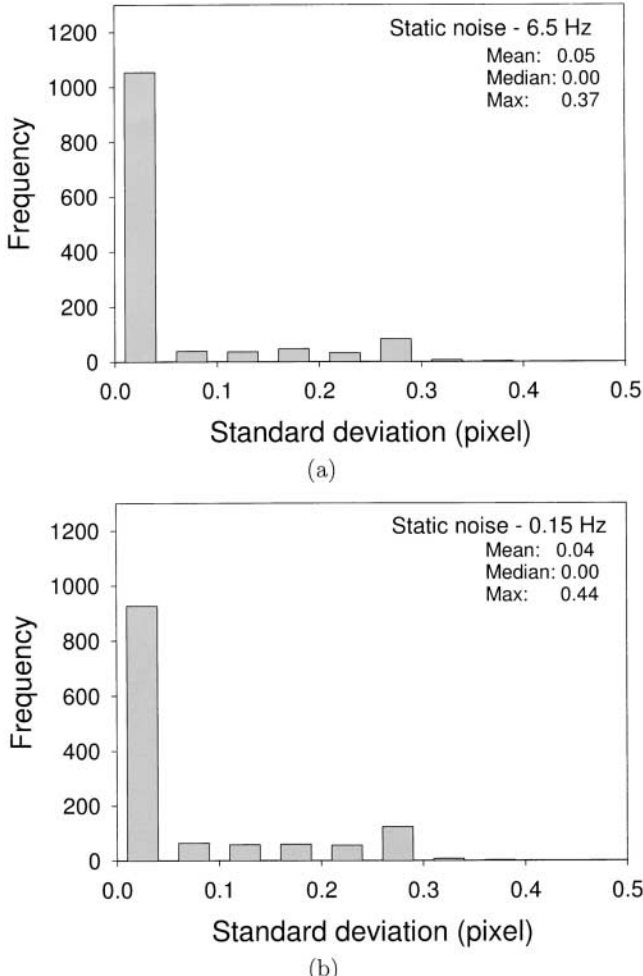


Fig. 6. Distribution of static noise at an acquisition rate of (a) 6.5 Hz and (b) 0.15 Hz.

Table 1. Positional accuracy, showing as standard deviations of ten repeated scans from the two ends (i.e., Begin and End) separated 0.9, 1.8, 2.7, and 3.6 m apart. The test was conducted for both forward and backward movements of the laser scanner assembly.

Scan distance	Standard deviation, mm			
	Forward		Backward	
m	Begin	End	Begin	End
0.9	0.46	0.48	0.50	0.48
1.8	0.41	0.36	0.51	0.42
2.7	0.42	0.45	0.45	0.51
3.6	0.48	0.57	0.46	0.52

tated 180°. We used a grid spacing of 1.5 mm in both x and y directions. We first corrected the shift and rotation in x and y between the two DEMs by using twelve ground check points. These ground check points were actual points of the soil surface that could be identified on both DEMs. They were distributed over the common area (approximately 0.45 by 2.8 m). The standard deviation of the matching points equaled 0.43 cell (0.65 mm) for the column and 0.31 cell (0.47 mm) for the row. It

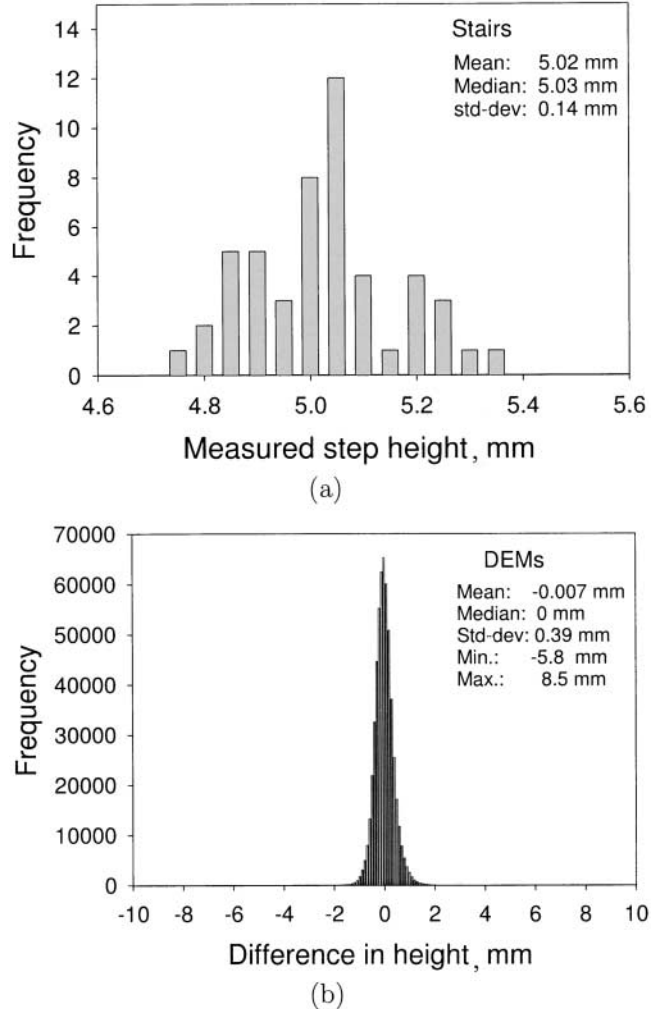


Fig. 7. Accuracy analysis of the laser scanner showing (a) absolute accuracy from the distribution of measured heights obtained using a stairlike shape object with 5-mm high steps; and (b) relative accuracy from the distribution of height differences from two digital elevation models (DEMs) of the same soil surface.

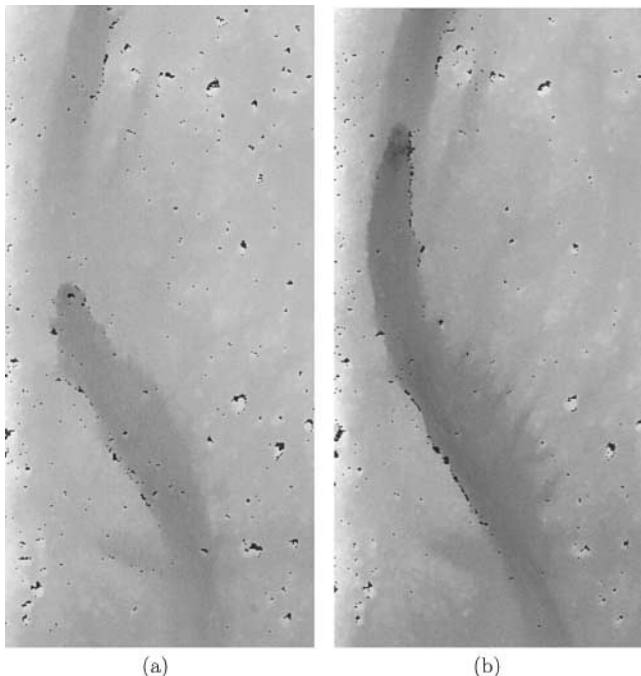


Fig. 8. Successive laser-scanned surface topography displaying the progression of a head cut from an area 35 cm wide by 70 cm long. Heights are represented in gray levels with darker tones for lower elevations (maximal height range: 44 mm). The black areas are missing values because of the shadow effect.

shows there is low spatial distortion in the horizontal plane.

We then adjusted the general slope of the DEMs to correct for the vertical shift because of the change in position of the scanner. We computed the differences in height for each pixel (Fig. 7b). The standard deviation of the measurement equals 0.39 mm. This value is close to the vertical resolution, showing the operational performance of the system is optimal. The bell-shaped curve is symmetric, without bias. The large differences between the DEMs occurred locally at the boundary of some roughness elements protruding from the surface (aggregates). At those locations, a slight positional shift gave rise to large differences in height.

Practical Limitations

Shadow Effect

We mentioned in the introduction that all triangulation-based laser scanners are sensitive to the shadow effect. This shadow effect is because of the obstruction of the light path by a roughness element. For the instantaneous-profile laser scanner, a roughness element can block the laser beam both in x and y directions.

The x -direction shadow effect is caused by the blockage of the laser light before it reaches the target point. This shadow effect was not present in the point laser scanners because the illumination of the surface was always vertical. This shadow effect is decreased by the use of two lasers illuminating the surface with opposite incident angles. The y -direction shadow effect, the blockage of the laser light from the camera viewing

angle, can be reduced by scanning the surface in opposite directions or using two cameras.

Contrast of Light

The use of two lasers to generate the laser line and a red filter on the camera lens increases the contrast between the laser line and the background. The contrast is sufficient for indoor use under normal lighting. Shading is necessary when using the scanner outdoors during daylight hours.

Surface Material

The material composing the surface must reflect the laser light for the CCD camera to detect the laser line. Therefore, the laser scanner cannot be used on surfaces that absorb the red light. It cannot be used on surfaces with transparent or translucent material (ponded areas). If the material has a strong specular reflection, such as metals, the pattern of the laser line will be affected.

Temperature

Among all the components, the camera is the most temperature sensitive. Its operation temperature ranges from 5 to 40°C. Temperature rarely causes a problem in laboratory settings. In field situations, the use of a silver colored reflective cover to provide shading can alleviate temperature related problems in hot summer days.

Application Example

Surface roughness affects numerous physical processes. Some physical processes, such as erosion, also cause changes in surface micromorphology. For soil erosion studies, microtopographic measurements can be used to quantify detachment and deposition. Because the instantaneous-profile laser scanner maps accurately the spatial variations, flow paths and depression volumes can be computed. By scanning the same area successively, temporal changes can also be assessed. As an example, Fig. 8 shows the morphological features from a laboratory rainfall simulation study. With such DEMs, the microerosional changes occurring during the rain can be quantified. With the good spatial resolution and accuracy of the instrument, precise volume changes can be calculated.

CONCLUSIONS

The instantaneous-profile laser scanner was designed to measure soil surface microtopography with a submillimeter resolution in all directions. The key improvement lies in the instantaneous measure of height changes along a profile. Moving the carriage along a single rail reduces the overall size. Its performance equals previous laser scanners in terms of accuracy and resolution and but far exceeds their data acquisition rate. It can be used in various conditions, both indoor and outside in the field.

REFERENCES

- Bertuzzi, P., J.M. Caussignac, P. Stengel, G. Morel, J.Y. Lorendeau, and G. Pelloux. 1990. An automated, noncontact laser profile meter for measuring soil roughness *in situ*. *Soil Sci.* 149:169–178.
- Buiten, H.J. 1993. Geometrical and mapping aspects of remote sensing. p. 297–321. *In* H.J. Buiten and J.G.P.W. Clevers (ed.) *Land observation by remote sensing: Theory and applications*. Gordon and Breach science, Amsterdam.
- Flanagan, D.C., C. Huang, L.D. Norton, and S.C. Parker. 1995. Laser scanner for erosion plot measurements. *Trans. ASAE* 38:703–710.
- Huang, C., and J.M. Bradford. 1990. Portable laser scanner for measuring soil surface roughness. *Soil Sci. Soc. Am. J.* 54:1402–1406.
- Huang, C., I. White, E. Thwaite, and A. Bendeli. 1988. A noncontact laser system for measuring soil surface topography. *Soil Sci. Soc. Am. J.* 52:350–355.
- Imagine Optic. 2001. PHLINE [online]. Available at <http://www.imagine-optic.com> (verified 8 Aug. 2002).
- Kamphorst, E. 2000. Measurement and estimation methods of maximum depression storage on tilled soils. (In French, with English summary.) Ph.D. dis., Institut National Agronomique Paris, Grignon, France.
- Kuipers, H. 1957. A reliefmeter for soil cultivation studies. *Netherlands J. Agric. Sci.* 5:255–262.
- Rice, C., B.N. Wilson, and M. Appleman. 1988. Soil topography measurements using image processing techniques. *Comput. Electron. Agric.* 3:97–107.
- Römkens, M.J.M., and J.Y. Wang. 1987. Soil roughness changes from rainfall. *Trans. ASAE* 30:101–107.
- Warner, W.S. 1995. Mapping a three-dimensional soil surface with handheld 35 mm photography. *Soil Tillage Res.* 34:187–197.
- Whalley, W.B., and B.R. Rea. 1994. A digital surface roughness meter. *Earth Surf. Processes Landforms* 19:809–814.
- Wilson, B.N., R.B. Leaf, and B.J. Hansen. 2001. Microrelief meter for field topography measurements. *Trans. ASAE* 44:289–295.
- Zribi, M., V. Ciarletti, O. Taconet, J. Paillé, and P. Boissard. 2000. Characterization of the soil structure and microwave backscattering based on numerical three-dimensional surface representation: Analysis with a fractional Brownian model. *Remote Sens. Environ.* 72:159–169.